

Supporting Information

Insights into the mechanism of electrocatalysis of oxygen reduction reaction by a porphyrinic metal organic framework

**M. Lions, J.-B. Tommasino, R. Chattot, B. Abeykoon, N. Guillou, T. Devic,
A. Demessence, L. Cardenas, F. Maillard and A. Fateeva**

Univ. Grenoble Alpes, LEPMI, F-38000 Grenoble, France

CNRS, LEPMI, F-38000 Grenoble, France

*Université de Lyon, Université Claude Bernard Lyon 1, Laboratoire des Multimatériaux et Interfaces, UMR
CNRS 5615, 43 Bd du 11 Novembre 1918, 69622 Villeurbanne, France*

*Institut Lavoisier, UMR CNRS 8180, Université de Versailles Saint-Quentin-en-Yvelines, Université Paris-
Saclay, 45 avenue des Etats-Unis, 78035 Versailles cedex, France*

*Institut des Matériaux Jean Rouxel (IMN), UMR 6502, Université de Nantes, CNRS, 2 rue de la Houssinière,
BP32229, 44322 Nantes cedex 3, France*

*Institut de Recherches sur la Catalyse et l'Environnement de Lyon, Université Claude Bernard Lyon 1, CNRS
UMR 5256, Villeurbanne, France*

Contents

Section 1	Chemicals and Instrumentations	3
Section 2	Electrochemical characterizations in liquid electrolyte	5
Section 3	Synthesis	6
Section 4	Characterisations of Co-Al-PMOF	7
Section 5:	Microscopy characterisations	14
Section 6:	Electrochemical data	16

Section 1: Chemicals and Instrumentations

All chemicals were obtained from commercial sources and used without further purification.

The tetrakis(4-carboxyphenyl)porphyrin was purchased at TCI chemicals. Vulcan XC72-supported Pt nanoparticles with a weight fraction of 20 % (TEC10V20E) were purchased from Tanaka Kikinzoku (TKK), and used as-received.

Powder X-Ray diffraction (PXRD) was performed on a PANalytical XpertPro MRD diffractometer with a Cu K α 1 radiation ($\lambda = 1.540598 \text{ \AA}$) used with 40 kV and 30 mA settings in θ/θ mode, reflection geometry. High resolution powder X-ray diffraction data of Co-Al-PMOF were measured at room temperature using a Bruker D8 Advance diffractometer with a Debye-Scherrer geometry, in the 2θ range 3-90 °. The D8 system is equipped with a Ge(111) monochromator producing Cu K α 1 radiation ($\lambda = 1.540598 \text{ \AA}$) and a LynxEye detector.

Scanning Electron Microscopy and Energy Dispersive Spectroscopy analysis was performed by scanning electron microscopy on FEI Quanta 250 FEG and Zeiss Merlin Compact microscopes in the microscopy center of Lyon1 University. Samples were mounted on stainless pads and sputtered with $\sim 2 \text{ nm}$ of carbon to prevent charging during observation.

Transmission Electron Microscopy of the different electrocatalytic materials was performed on a JEOL 2010 TEM equipped with a LaB6 apparatus operating at 200 kV (point to point resolution of 0.19 nm).

Thermogravimetric analysis (TGA) was performed with a TGA/DSC 1 STARe System from Mettler Toledo. Around 5 mg of sample is heated at a rate of $10 \text{ K}\cdot\text{min}^{-1}$ from 25 to 800 °C, in a 70 μL alumina crucible, under air atmosphere ($20 \text{ mL}\cdot\text{min}^{-1}$).

Infrared spectroscopy was performed with a Nicolet 380 FT-IR spectrometer coupled with the Attenuated Total Reflectance (ATR) accessory.

Mass spectrometry was performed in the Centre Commun de Spectrométrie de Masse (CCSM) in Lyon 1 University on a MicrOTOFQ II – Bruker in electrospray Ionisation mode (ESI)

Specific surface areas were measured by N $_2$ adsorption and desorption at 77.3 K using a BEL Japan Belsorp Mini apparatus volumetric adsorption analyzer. The sample was pre-activated under vacuum at 160 °C prior to sorption measurement. The BET surface calculations was performed using points at the pressure range $0 < P/P^0 < 0.10$

X-ray photoelectron spectroscopy (XPS) experiments were carried out on a commercial KRATOS Axis Ultra DLD spectrometer using monochromated Al K α source ($h\nu = 1486.6$ eV, 150 W), a pass energy of 20 eV, a hybrid lens mode at ultra-high vacuum ($P < 10^{-9}$ mbar). Scan survey was done at energy of 160 eV and the Co2p element at 20 eV. The peak positions were referenced to the aromatic carbon atoms components of the C1s band at 284.6 eV. Shirley background subtraction and peak decomposition using Voigt function were performed with the CASA XPS processing program.

Section 2: Electrochemical characterizations in liquid electrolyte

All the glassware used in this study was cleaned by > 12 hours immersion in a $\text{H}_2\text{SO}_4/\text{H}_2\text{O}_2$ mixture and thoroughly rinsed with MQ-grade water (Millipore, $18.2 \text{ M}\Omega \text{ cm}$, 1-3 ppm TOC) before use. The electrolyte ($0.1 \text{ M H}_2\text{SO}_4$) was prepared from MQ-grade water and H_2SO_4 (Suprapur[®], Merck). The potentiostat was a SP300 from Biologic. It was operated in "CE to Ground" mode, which allows the user to control the potential of several working electrodes connected together. A rotating ring disk electrode (RRDE) assembly (Pine instrument) composed of a glassy carbon disk (5 mm outer diameter (AFED050P040PT)) and a platinum ring (AFE6R1PT, 6.5 mm inner diameter and 7.5 mm outer diameter) was used. The collection efficiency (N) for this electrode was 0.25. The counter-electrode was a glassy carbon plate, and the reference electrode – a reversible hydrogen electrode (Hydroflex, Gaskatel GmbH) - connected to the cell *via* a Luggin capillary. The rotation rate was controlled by a Pine Instrument system (AFASRE).

To prepare the working electrodes, a suspension containing the catalytic powders, Vulcan XC72 (Cabot), Nafion[®] solution (Electrochem. Inc.), isopropanol and deionized water (MQ-grade, Millipore, $18.2 \text{ M}\Omega \text{ cm}$, 1-3 ppm TOC) was made. After sonication for 15 minutes, $10 \mu\text{L}$ of the suspension was pipetted onto the glassy carbon disk (AFED050P040GC, Pine Instruments), and sintered for 5 minutes at $T = 110 \text{ }^\circ\text{C}$ to ensure evaporation of the solvents. Cyclic voltammograms were recorded in Ar-saturated electrolyte between 0.05 V and 1.23 V *vs.* the reversible hydrogen electrode (RHE) with a potential sweep rate of 0.050 V s^{-1} . The electrocatalytic activity for the oxygen reduction reaction was measured in O_2 -saturated $0.1 \text{ M H}_2\text{SO}_4$ solution (20 minutes of purging by oxygen > 99.99 %, Messer) by linearly sweeping the potential from 0.18 to 1.05 V *vs.* RHE at a potential sweep rate of 5 mV s^{-1} and at different rotational speeds (400, 900, 1600, and 2500 rpm).

Section 3: Synthesis

CoTCPP preparation procedure

Cobalt tetrakis(4-carboxyphenyl)porphyrin was prepared following a classic procedure. First the free base Meso-tetra(4-carboxyphenyl)porphine tetramethyl ester was prepared by Adler Longo method¹ starting from pyrrole and methyl 4-formyl benzoate. Cobalt insertion was performed in quantitative yield by refluxing this porphyrin with 3 equivalents of cobalt (II) acetate tetrahydrate in DMF for 4 hours. The cobalt tetra(4-carboxyphenyl)porphine tetramethyl ester was recovered by precipitation in DMF/water mixture and the ester functions were hydrolysed to carboxylic acid by refluxing overnight in a mixture of THF and aqueous NaOH solution (100 equivalents of NaOH). The desired compound was precipitated by careful addition of 2M HCl solution, filtered and dried under vacuum. This gave the cobalt tetrakis(4-carboxyphenyl)porphyrin CoTCPPX ($X = OH^-$) in a quantitative yield.

Metal Organic Framework Co-Al-PMOF preparation procedure

H₂-Al-PMOF was prepared as described in the literature² and was activated overnight under vacuum at 160 °C. Cobalt (II) acetate tetrahydrate (42 mg, 0.17 mmol) was added to 25 mL of DMF and sonicated for 10 minutes. To this mixture 100mg (0.11 mmol) of activated H₂-Al-PMOF was added, the suspension was stirred and then left to react at 120 °C in a programmable oven for 40 hours. After this time, the reaction mixture was cooled down and the sample was recovered by centrifuging at 6000 rpm and washing three times with DMF, water and acetone. The recovered solid was activated under vacuum at 160 °C overnight to give 85 mg of red powder (yield : 84 %).

Section 4: characterizations of Co-Al-PMOF and Co-TCPP

Rietveld analysis

Extractions from the peak positions, pattern indexing, difference Fourier calculations as well as Rietveld refinement were carried out with the TOPAS program³.

Similarities between powder patterns of the H₂-Al-PMOF and Co-Al-PMOF (Fig. 1) led us to suppose that the two compounds were isostructural. Unindexed lines observed on the powder pattern correspond to boehmite impurity and its structural model was introduced in the next steps of the Rietveld refinement. The structural model of an isotopic phase [Fe₁₀pzTCPP(Fe_{III}OH)₂]_n obtained from single crystal data⁴ was then used as a starting point of the Rietveld refinement of Co-Al-PMOF. Difference Fourier calculations allowed to localize unambiguously the Co cation at the centre of the porphyrin with a full occupancy, and three additional disordered water molecules. The final Rietveld plot (Figure S1) corresponds to satisfactory model indicator and profile factors (R_{Bragg} = 0.005, R_p = 0.013, RWP = 0.018). It involves the following structural parameters for Co-Al-PMOF: 4 atomic coordinates of the water molecules (atoms of the framework were fixed during the refinement), 2 occupancy factors, 1 thermal factor and 1 scale factor. The amount of boehmite was estimated at about 18.4 % weight.

Note: a better crystallised sample was used for Rietveld analysis, when in the sample used in electrocatalysis experiments the boehmite amount was calculated from TGA data and found to be 6% weight.

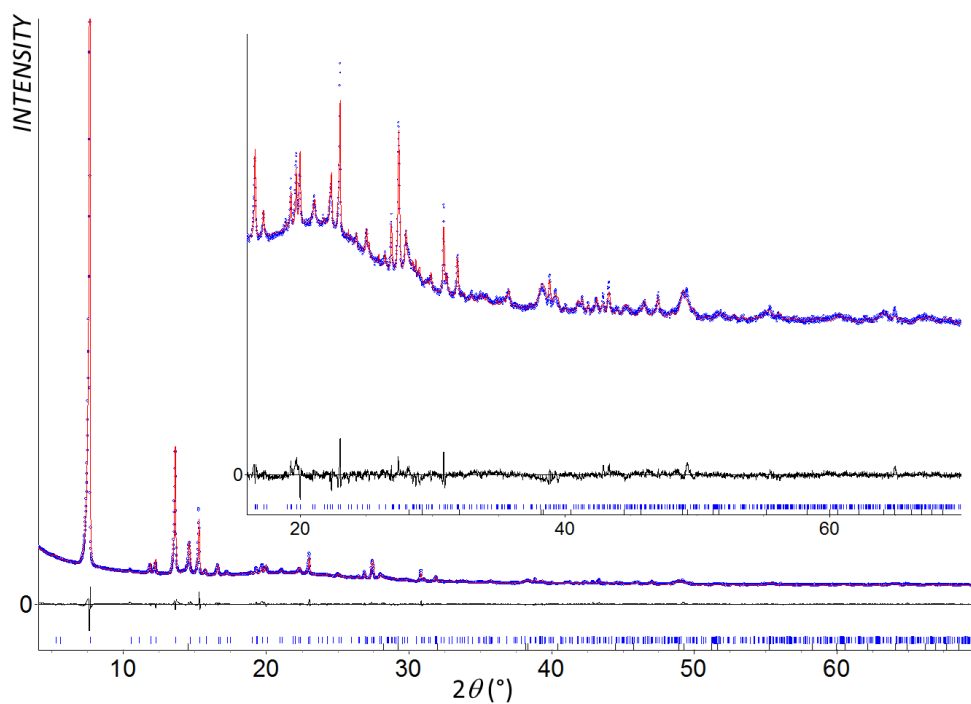


Figure S1. Plot showing the result of Rietveld analysis of Co-Al-PMOF. Blue circles: observed pattern, red line: calculated pattern, black line: difference between measured and calculated patterns.

PXRD analysis for CoTCPP

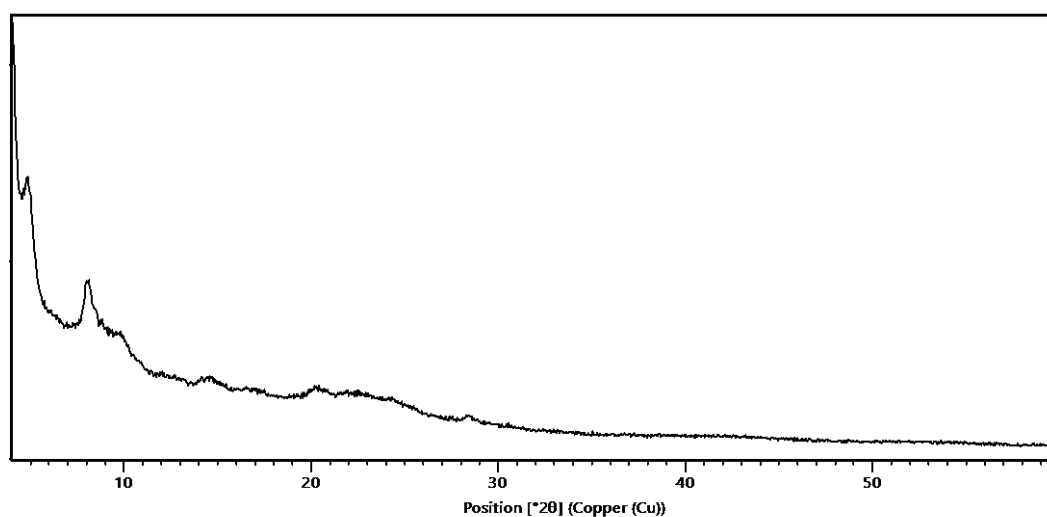


Figure S2. PXRD of CoTCPP.

UV-vis absorbance

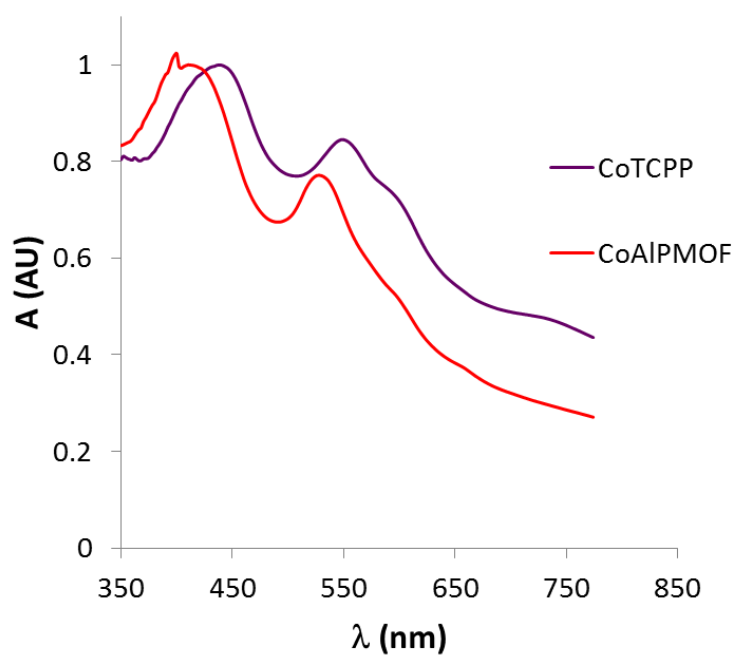


Figure S3. Solid state UV-vis absorbance spectra of CoTCPP and Co-Al-PMOF.

IR data

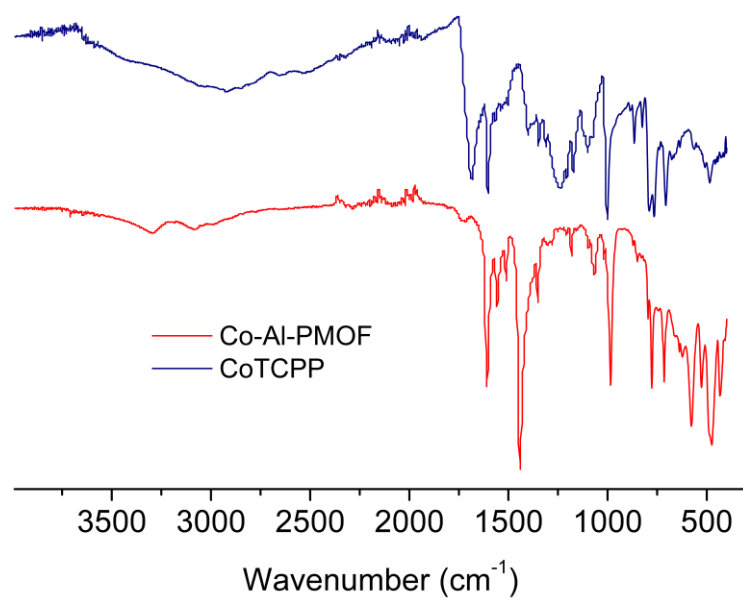


Figure S4. Infrared spectra of CoTCPP and Co-Al-PMOF.

XPS data

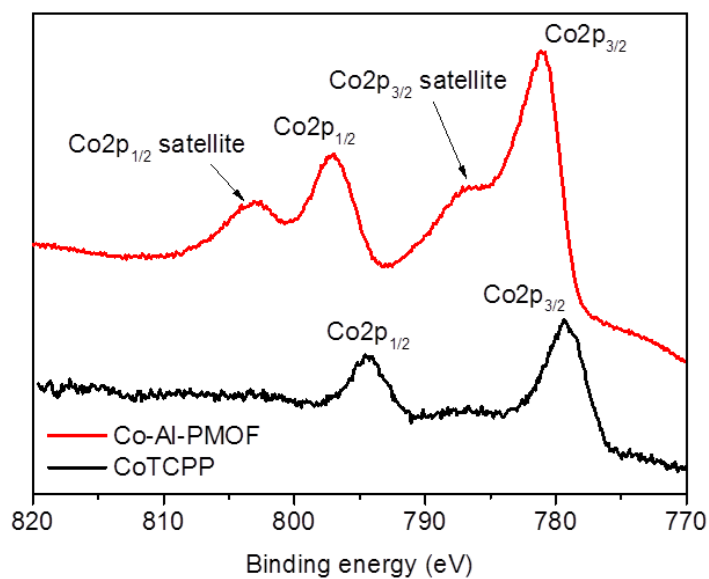


Figure S5. X-ray photoelectron spectra of Co-Al-PMOF and Co-TCPP compounds from Co₂p binding energies⁵

TGA of H₂-AIPMOF and Co-Al-PMOF

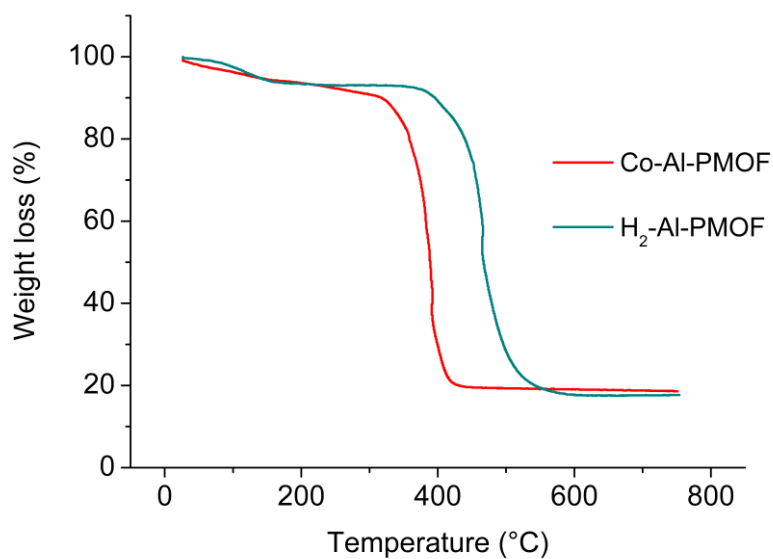


Figure S6. TGA curves for H₂-Al-PMOF and Co-Al-PMOF under air, heating rate: 10 °C per minute

Surface area measurement for Co-Al-PMOF

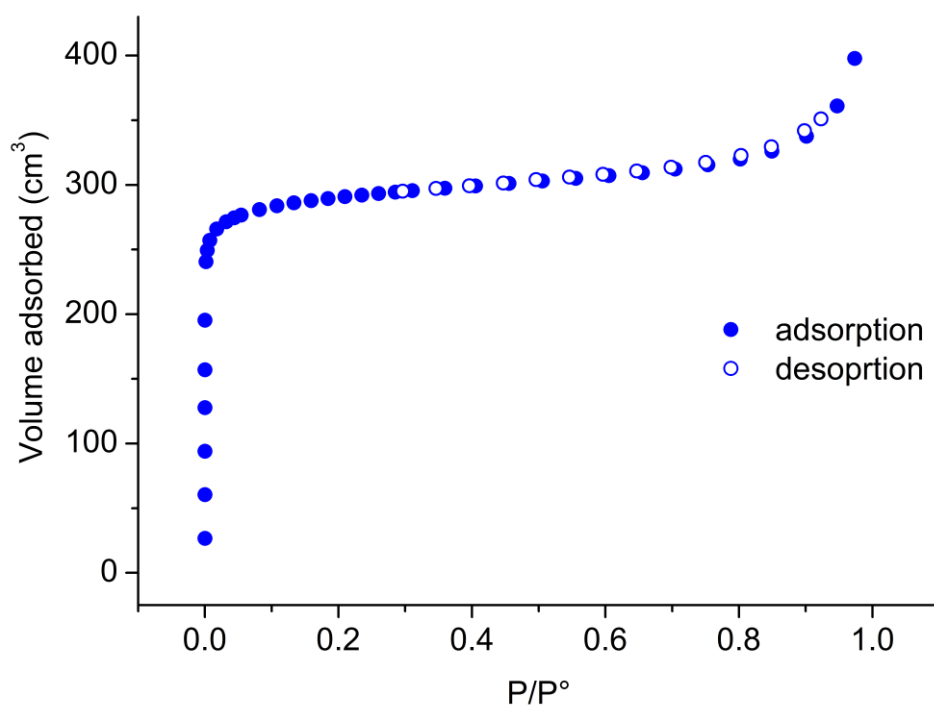


Figure S7. Nitrogen sorption isotherms for Co-Al-PMOF at -196 °C.

Stability check in 0.1M H₂SO₄

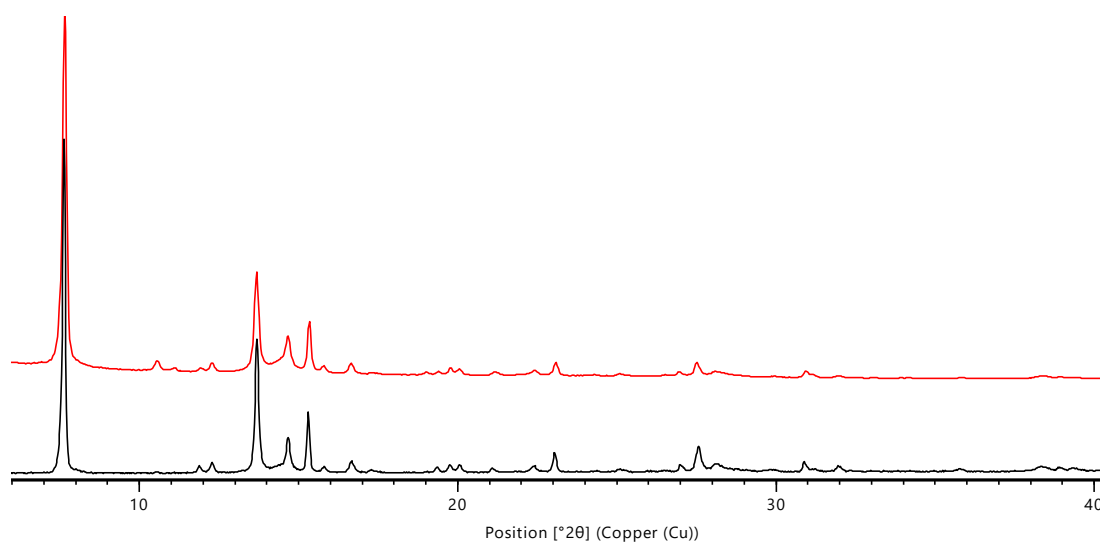


Figure S8. PXRD of Co-Al-PMOF before (black) and after stirring in 0.1M H₂SO₄ for 24 hours (red).

Mass spectrometry: the MOF sample was digested in 0.02 M NaOH solution for MS analysis

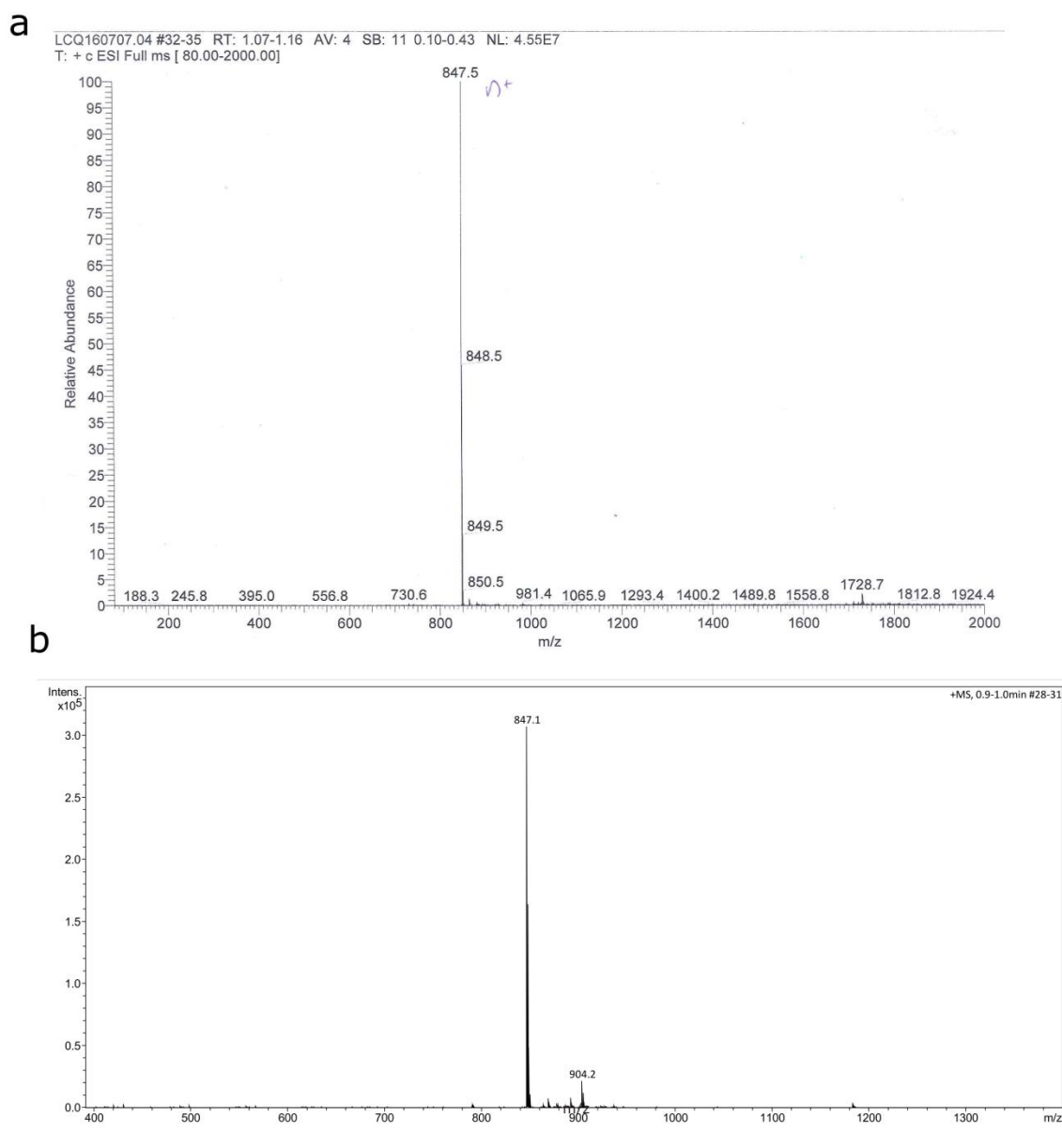


Figure S9. Mass spectrometry analysis for CoTCPP (a) and Co-Al-PMOF after dissolution in 0.02 M sodium hydroxide (NaOH) solution.

Scanning Electron Microscopy on Co-Al-PMOF, EDS analysis

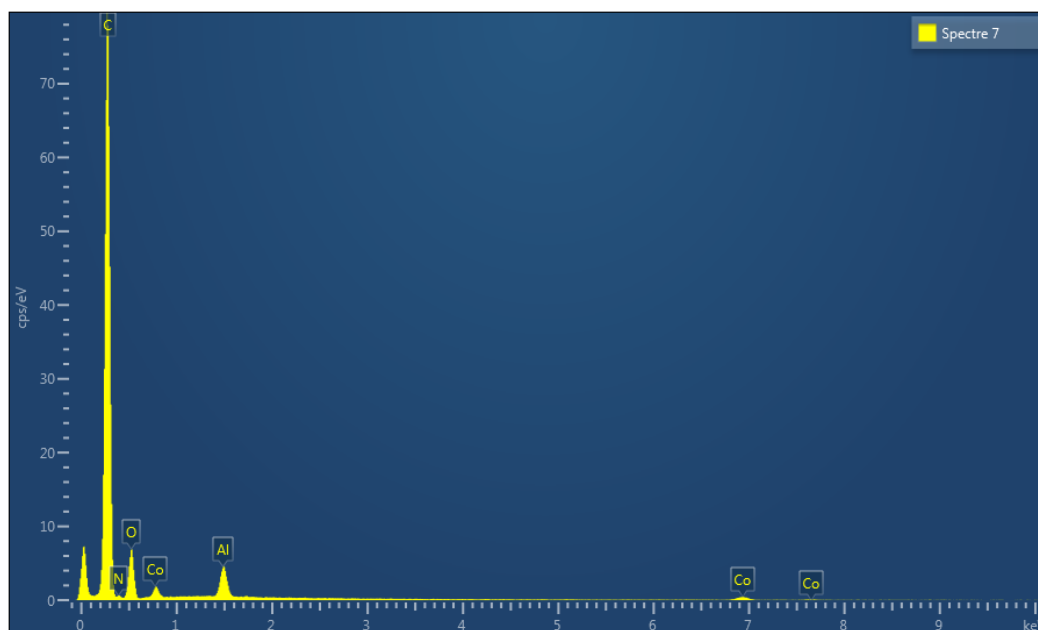


Figure S10. EDS analysis on Co-Al-PMOF

	Spectrum 1	Spectrum 2	Spectrum 3	Spectrum 4	Spectrum 5	Spectrum 6	Spectrum 7	Spectrum 8
Al atomic %	25.43	18.04	21.57	21.25	21.25	22.23	18.39	11.58
Co atomic %	10.51	8.22	8.61	11.18	10.2	9.77	8.25	6.29

Statistics	Al	Co
Maxi	25.43	11.18
Mini	11.58	6.29
Average	17.75	8.11
Standard deviation	4.09	1.59

Section 5: Microscopy characterisation of the electrodes and Co-Al-PMOF

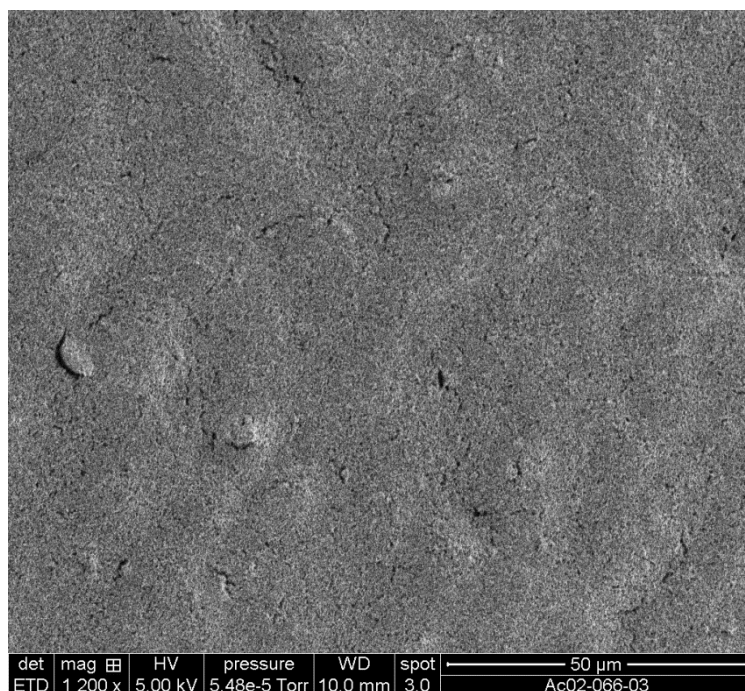


Figure S11. Scanning electron micrograph of Co-Al-PMOF containing electrode surface.

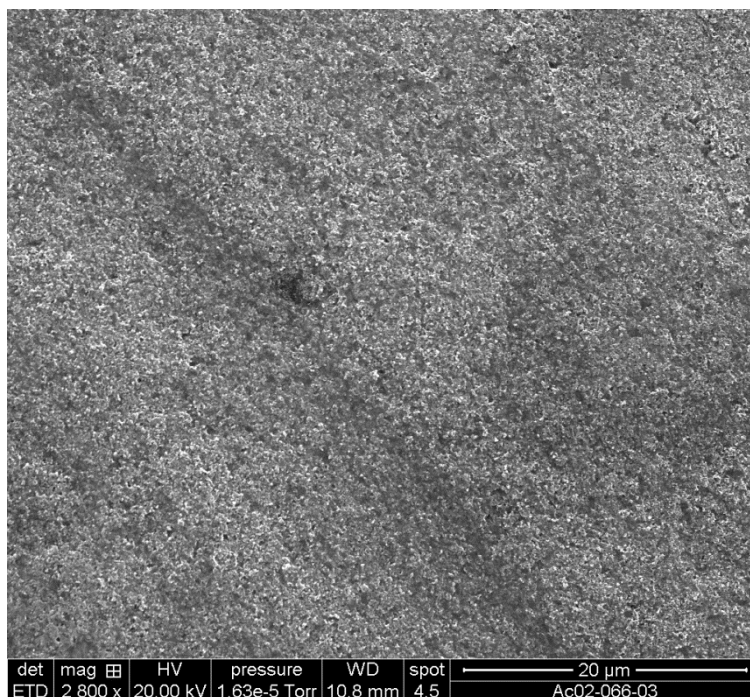


Figure S12. Scanning electron micrograph of CoTCPP containing electrode surface.

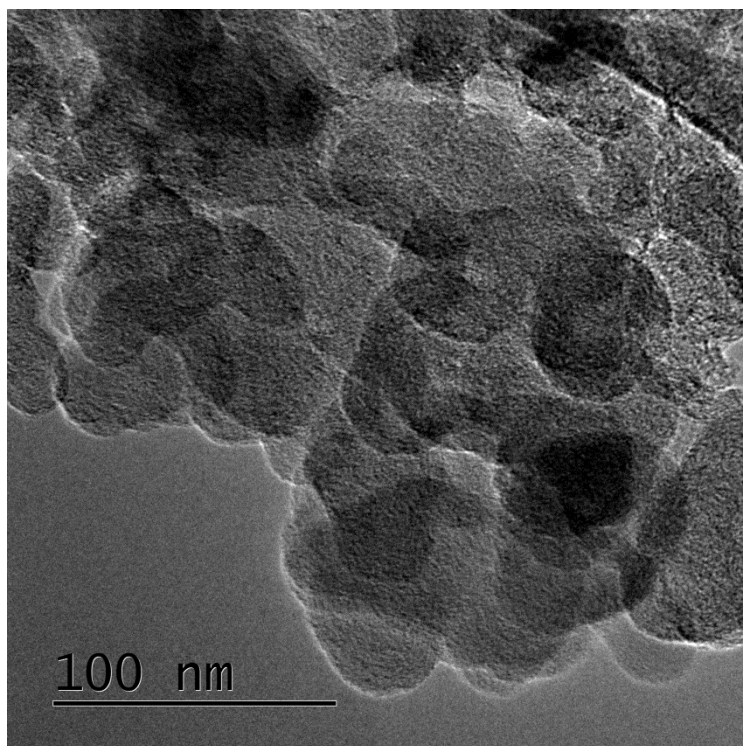


Figure S13. Transmission electron microscopy image of Co-Al-PMOF + Vulcan XC 72 .

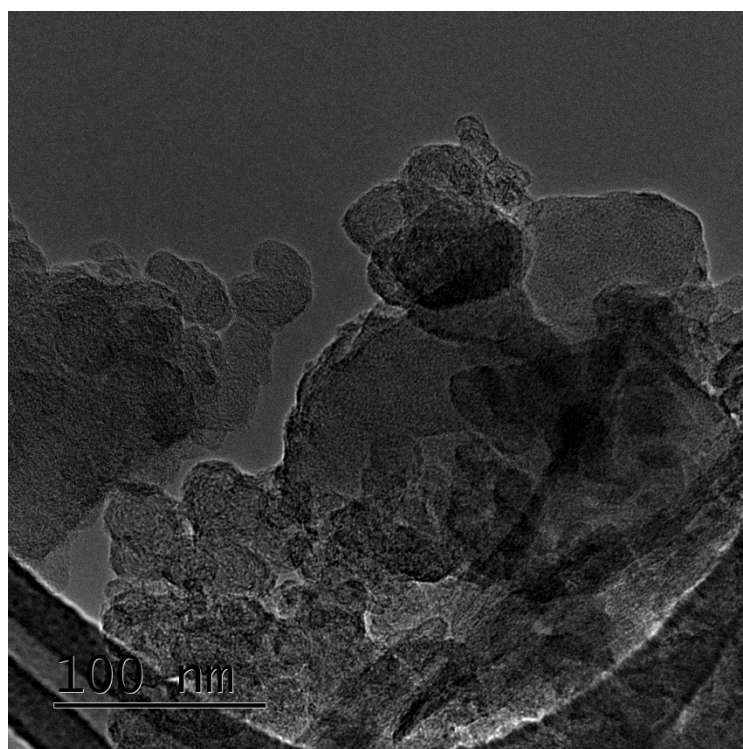


Figure S14. Transmission electron microscopy image of the electrode surface (scrubbed onto the TEM grid) containing Co-Al-PMOF + Vulcan XC72.

Section 6: Electrochemical data

Electrode preparation optimization

The MOF loading (weight percent) was optimized by preparing working electrodes with variable MOF/Vulcan ratios. Polarization curves were obtained, suggesting that ~60% weight of MOF gave optimal behaviour.

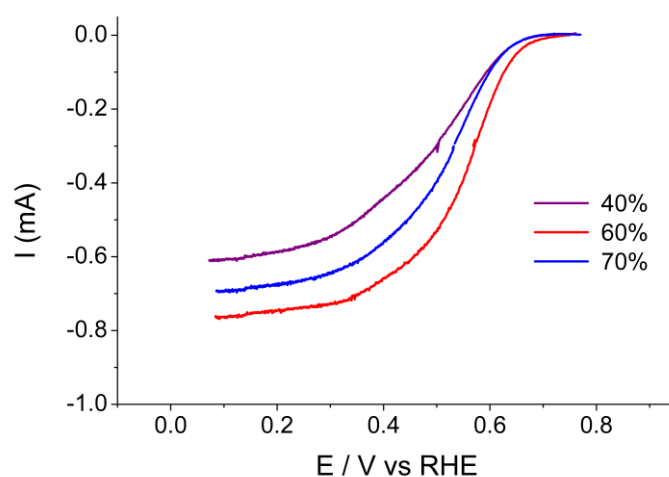


Figure S15. Linear voltammetry at rotating disc electrode (1600 rpm, 5 mV s^{-1}) composed of Vulcan XC72 + Nafion® + various Co-Al-PMOF contents in O_2 -saturated $0.1 \text{ M H}_2\text{SO}_4$.

Comparison of the ORR activity with the free base MOF (H_2 -Al-PMOF)

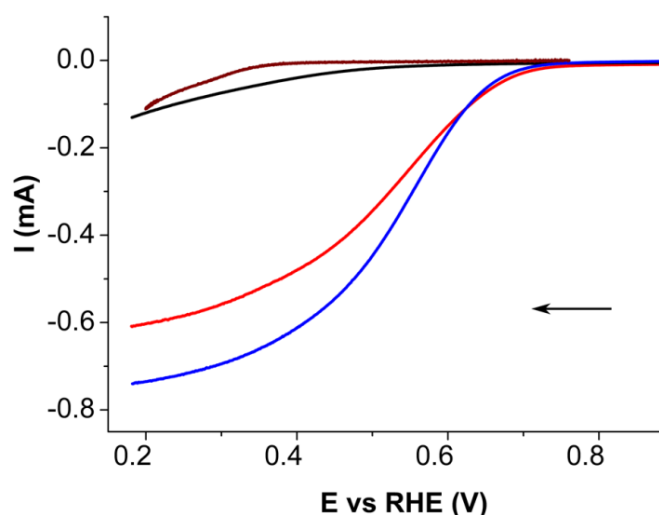


Figure S16 : linear sweep voltammograms of Vulcan + Nafion® (black), H_2 -Al-PMOF (wine), Co-Al-PMOF + Vulcan + Nafion® (red), CoTCPP + Vulcan + Nafion® (blue). The experiments were performed in O_2 -saturated $0.1 \text{ M H}_2\text{SO}_4$ at a potential sweep rate of 5 mV s^{-1} and $\omega = 1600$ revolutions per minute.

Limiting current at different rotation rates

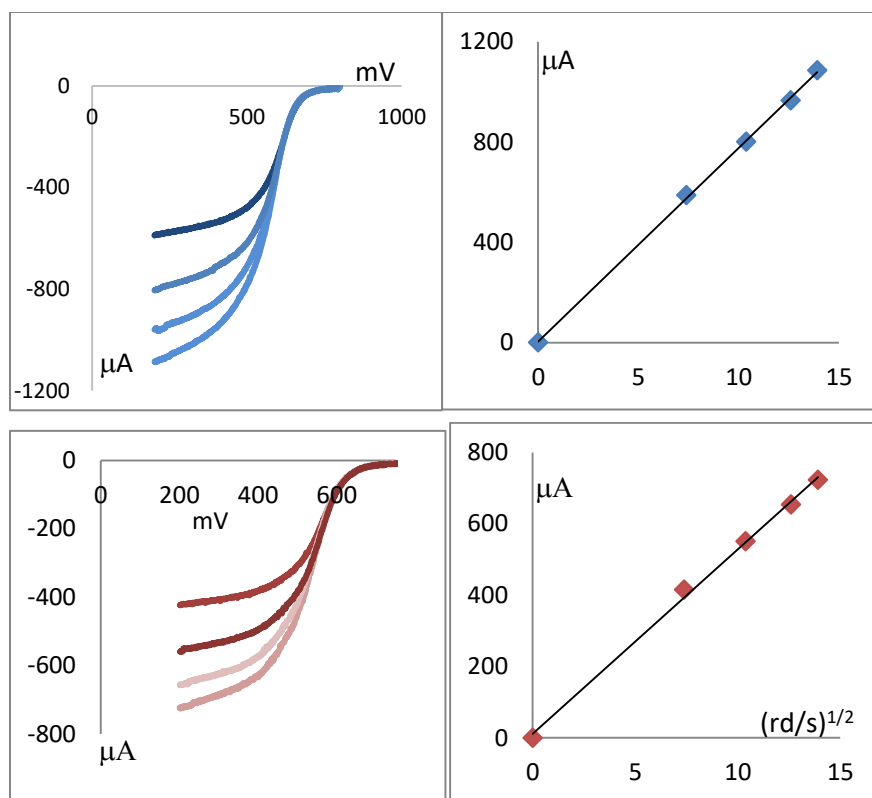


Figure S17. Linear voltammetry at variable rotation rate of the rotating disk electrode (RDE) and limiting current vs. square root of the rotation rate plots for: top: CoTCPP + Vulcan XC72 + Nafion[®], bottom: Co-Al-PMOF + Vulcan XC72 + Nafion[®], $\nu = 5 \text{ mV s}^{-1}$, O_2 -saturated $0.1 \text{ M H}_2\text{SO}_4$.

TOF calculations

For each current, the corresponding number of electrons per second was calculated by converting the coulombs per second in electrons per second. For the TOF calculation, all the Co sites were considered as active, in the MOF chemical formula: $\text{CoTCPPAl}_2\text{OH}_2$ therefore the number of electrons per second was divided by the number of active sites to get the final column in the TOF calculation.

For Co-Al-PMOF

E (V vs. RHE)	I (μA)	e^- per second	e^- per active site per second
0.65	72	$0.45 \cdot 10^{15}$	0.016
0.63	100	$0.62 \cdot 10^{15}$	0.022
0.60	150	$0.93 \cdot 10^{15}$	0.033
0.53	286	$1.77 \cdot 10^{15}$	0.063
0.5	344	$2.13 \cdot 10^{15}$	0.075
0.4	480	$2.98 \cdot 10^{15}$	0.105
0.3	565	$3.5 \cdot 10^{15}$	0.124

For CoTCPP

E (V vs. RHE)	I (μ A)	e^- per second	e^- per active site per second
0.65	63.6	$0.394 \cdot 10^{15}$	0.014
0.63	96.6	$0.599 \cdot 10^{15}$	0.02
0.60	164	$1.0 \cdot 10^{15}$	0.036
0.53	368	$2.28 \cdot 10^{15}$	0.081
0.5	446	$2.76 \cdot 10^{15}$	0.115
0.40	610	$3.78 \cdot 10^{15}$	0.135
0.30	694	$4.3 \cdot 10^{15}$	0.154

RRDE experiments

In this set up, the potential of the platinum (Pt) ring electrode was set at $E = 1.25$ V vs. RHE to detect any hydrogen peroxide (H_2O_2) that may have been generated thereby allowing ascertaining the number of electrons exchanged during the process. The collection efficiency (N) for this electrode was 0.25.

The typical expected values of n_{e^-} is between 2 and 4 corresponding to two extreme cases, a value of 4 means that all the reacting oxygen (O_2) molecules are reduced into water (H_2O), whereas $n_{e^-} = 2$ means that the reduction of O_2 molecule proceeds only to H_2O_2 , which escapes from the catalyst layer without being reduced. In the first case, the H_2O_2 molar ratio $X_{H_2O_2}$ is 0 %, in the second case $X_{H_2O_2} = 100$ %.

Equations S1-S3 were used to determine the average number of exchanged electrons during ORR, IR and ID represent ring and disk currents respectively.

$$I_{2e^-} = I_R / N \quad \text{Equation (S1)}$$

$$I_D = I_{2e^-} + I_{4e^-} \quad \text{Equation (S2)}$$

$$\frac{I_D}{n_{e^-}} = \frac{I_{2e^-}}{2} + \frac{I_{4e^-}}{4} \quad \text{Equation (S3)}$$

The two- and four-electron disc currents are I_{2e^-} (H_2O_2) and I_{4e^-} (H_2O), respectively. The current related to the series reaction pathway ($O_2 \rightarrow H_2O_2 \rightarrow H_2O$) is assumed to be negligible, or included in the four-electron disc current. Hence, the number of exchanged electrons n_{e^-} is a function of the ring and disk currents:

$$n_{e^-} = \frac{4I_D}{I_D + I_R/N} \quad \text{Equation (4)}$$

Cyclic voltammetry in presence of H_2O_2

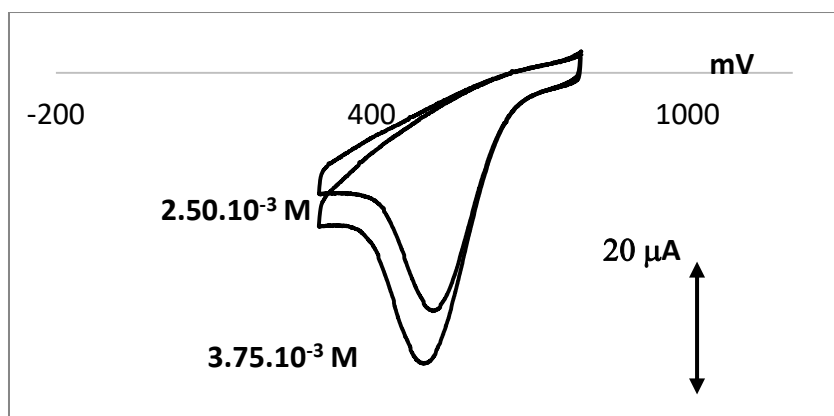


Figure S18. Cyclic voltammogram at 5 mV s^{-1} in Ar -saturated $0.1\text{M } \text{H}_2\text{SO}_4$: Co-Al-PMOF in presence of different concentrations of H_2O_2

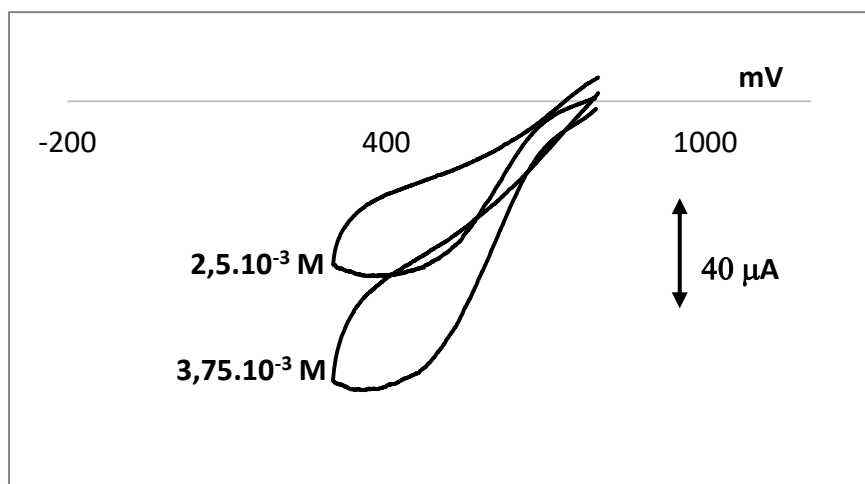


Figure S19. Cyclic voltammogram at 5 mV s^{-1} in Ar -saturated $0.1\text{M } \text{H}_2\text{SO}_4$: CoTCCP in presence of different concentrations of H_2O_2 .

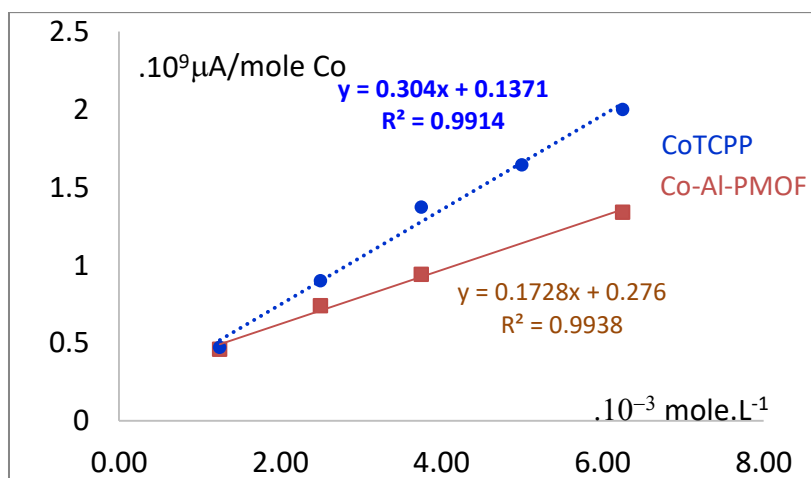


Figure S20. Normalised current per mole of Co sites for CoTCCP (blue) and Co-Al-PMOF (brown) for different concentrations of H_2O_2 .

RRDE experiments with the cobalt porphyrin bearing ester functions instead of the carboxylic acid (*tetramethyl 4,4',4'',4'''-(porphyrin-5,10,15,20-tetrayl)tetrabenzoate*).

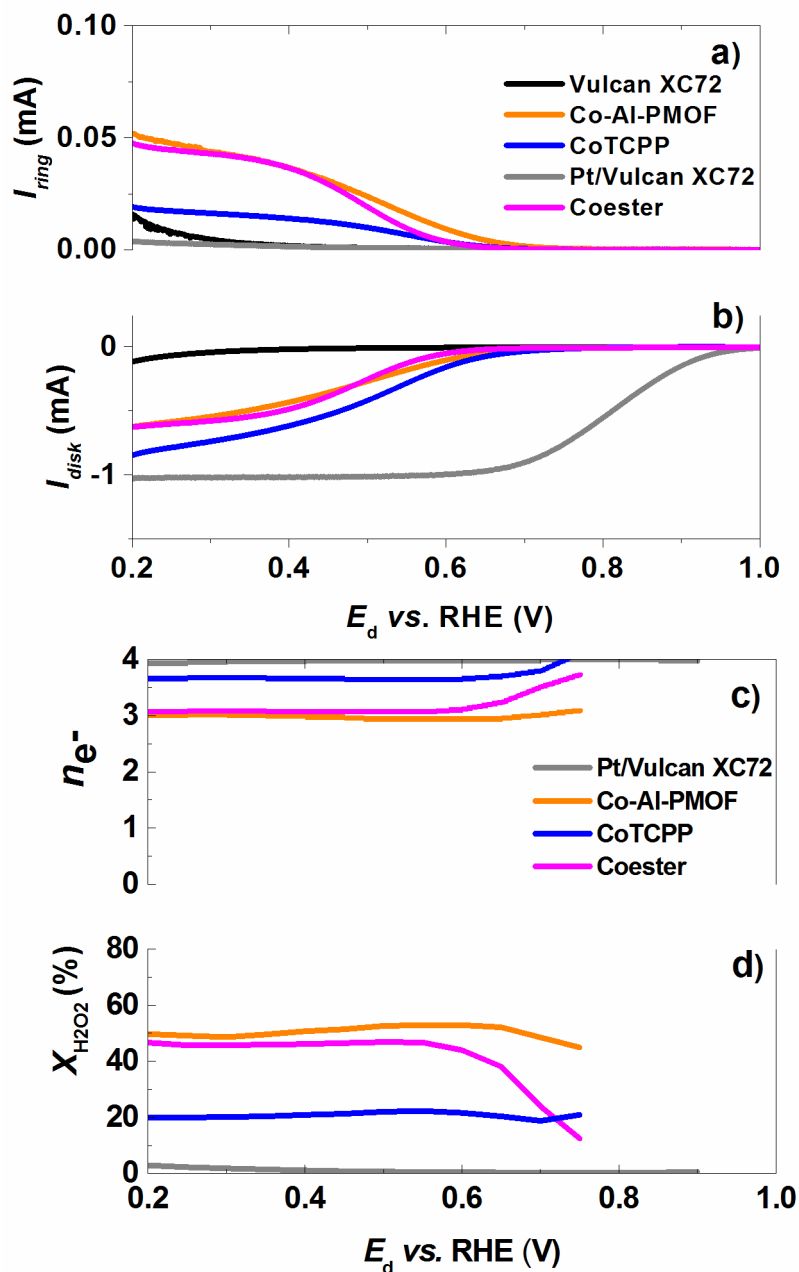


Figure S21. RRDE experiments: (a) ORR polarization curves on the glassy carbon disc coated with different catalytic materials and (c) hydrogen peroxide oxidation curves on the platinum ring electrode. (b) and (d) refer to the number of exchanged electrons and to the molar fraction of hydrogen peroxide produced during the ORR, respectively. Other conditions: rotation rate 1600 rpm; 0.1 M H_2SO_4 , temperature 25 ± 1 °C, catalysts loading $2.4 \cdot 10^{-7}$ mol cm^{-2} for Co-based materials and 100 μg_{powder} cm^{-2} for Vulcan XC72 and 20 wt. % Pt/Vulcan XC72 (TEC10V20E from TKK).

References

1. A. D. Adler, F. R. Longo, J. D. Finarelli, J. Goldmacher, J. Assour and L. Korsakoff, *J. Org. Chem.*, 1967, 32, 476-476.
2. A. Fateeva, P. A. Chater, C. P. Ireland, A. A. Tahir, Y. Z. Khimyak, P. V. Wiper, J. R. Darwent and M. J. Rosseinsky, *Angew. Chem. Int. Ed.*, 2012, 51, 7440-7444.
3. F. R. Nikkuni, B. Vion-Dury, L. Dubau, F. Maillard, E. A. Ticianelli and M. Chatenet, *Appl. Catal. B.*, 2014, 156-157, 301-306.
4. V. Goellner, C. Baldizzone, A. Schuppert, M. T. Sougrati, K. J. J. Mayrhofer and F. Jaouen, *Phys. Chem. Chem. Phys.*, 2014, 16, 18454-18462.
5. L. Dubau and F. Maillard *Electrochem. Commun.*, 2016, 63, 65-69.